Journal of Geochemical Exploration 125 (2013) 8–19

Contents lists available at SciVerse ScienceDirect

Journal of Geochemical Exploration

journal homepage: www.elsevier.com/locate/jgeoexp

Numerical modeling of fluid pressure regime in the Athabasca basin and implications for fluid flow models related to the unconformity-type uranium mineralization

Guoxiang Chi [a,*], Sean Bosman [b], Colin Card [b]

[a] Department of Geology, University of Regina, 3737 Wascana Parkway, Regina, SK, Canada S4S 0A2
[b] Saskatchewan Geological Survey, 200-2101 Scarth Street, Regina, SK, Canada S4P 2H9

ARTICLE INFO

Article history:
Received 31 March 2012
Accepted 29 October 2012
Available online 8 November 2012

Keywords:
Athabasca basin
Unconformity-type
Uranium deposits
Basinal fluids
Fluid flow
Overpressure

ABSTRACT

Various fluid-flow models have been suggested for the formation of unconformity-type uranium deposits in the Athabasca basin, including fluid flow driven by fluid overpressure, topographic relief, fluid density variation due to temperature or salinity change, and tectonic deformation. In order to evaluate the fluid-flow mechanisms responsible for mineralization, it is necessary to know the distribution and evolution of fluid pressure during the history of the basin. A numerical modeling study of the development of fluid overpressure due to disequilibrium sediment compaction was carried out, and the results suggest that no significant fluid overpressure was developed in the basin throughout the sedimentation history. Fluid flow related to sediment compaction was very slow and the temperature profile was undisturbed, implying that if compaction-driven flow was responsible for mineralization, the sites of mineralization would not show a thermal anomaly. The development of near-hydrostatic pressure regime in the Athabasca basin may have facilitated circulation of oxidizing fluids from the shallow part of the basin into the basal part, favoring the formation of unconformity-type uranium deposits, as opposed to other sedimentary basins where elevated fluid overpressures within the lower part of the basin may have prevented downward infiltration of oxidizing fluids, limiting uranium mineralization to the upper part of the basin.

1. Introduction

The Athabasca basin in northern Saskatchewan and Alberta hosts the world's largest high-grade uranium deposits, which are generally located near the unconformity between late Paleoproterozoic to Mesoproterozoic sedimentary rocks of the Athabasca Group and Archean to Paleoproterozoic metamorphic rocks in the basement (Jefferson et al., 2007; Kyser and Cuney, 2008). It is generally agreed that the mineralizing fluids were brines derived from the basin (e.g., Alexandre et al., 2005; Cuney et al., 2003; Derome et al., 2005; Kyser et al., 2000; Mercadier et al., 2012; Richard et al., 2011), although it is uncertain whether uranium was derived from the basin (Fayek and Kyser, 1997; Hoeve et al., 1980; Kotzer and Kyser, 1995; Kyser et al., 2000) or from the basement (Cuney et al., 2003; Dahlkamp, 1978; Hetch and Cuney, 2000; Richard et al., 2010). Various fluid-flow models related to uranium mineralization have been proposed or implied in previous studies (Chi et al., 2011), including large-scale convection related to thermal gradient (Boiron et al., 2010; Hoeve and Sibbald, 1978; Raffensperger and Garven, 1995) and deposit-scale convection related to heat anomaly associated with high heat conductivity of graphite (Hoeve and Quirt, 1984), gravity-driven flow (Alexandre and Kyser, 2012; Derome et al., 2005), compaction-driven flow (Hiatt and Kyser, 2007), and deformation-induced fluid flow (Cui et al., 2012). Some of these models assume that the fluid pressure in the basin was initially near hydrostatic (Cui et al., 2012; Raffensperger and Garven, 1995), some implied significant overpressure (Derome et al., 2005; Hiatt and Kyser, 2007), and some predict that the fluid pressure at the site of mineralization may have fluctuated between under-hydrostatic and near-lithostatic, either under a constant subhorizontal compressional stress regime (Tourigny et al., 2007), or in response to alternating compressional and extensional stress regimes (Cui et al., 2012). Therefore, the fluid pressure regime (hydrostatic, lithostatic, or intermediate) in the Athabasca basin during the history of sedimentation (1750 to <1541 Ma; Jefferson et al., 2007) remains unknown, which significantly hinders our understanding of the fluid-flow mechanisms responsible for uranium mineralization, as the time of primary uranium mineralization (mainly from ca. 1600 to 1500 Ma; Alexandre et al., 2009; Jefferson et al., 2007; Kyser and Cuney, 2008) largely overlaps with sedimentation in the basin. This paper addresses this problem through numerical modeling of the development of fluid overpressure (the difference between fluid pressures and hydrostatic values; Bethke, 1985) throughout the depositional history of the basin, using the software Basin2 (Bethke et al., 1993). We choose to use Basin2 because it is best suited for addressing the problem of disequilibrium sediment compaction (i.e., sediment compaction is hindered because pore fluid cannot escape rapidly enough due to low-permeability), which is the main cause of fluid overpressure in sedimentary basins (Swarbrick

* Corresponding author.
E-mail address: guoxiang.chi@uregina.ca (G. Chi).

0375-6742/$ – see front matter
http://dx.doi.org/10.1016/j.gexplo.2012.10.017

et al., 2002), and it can readily model the evolution of the basin with time. Numerical modeling of fluid flow has become increasingly important in understanding mineralization processes (Zhao et al., 2012), and various numerical models have been investigated for a given mineralization system, including unconformity-type uranium mineralization (Cui et al., 2012; Oliver et al., 2006; Raffensperger and Garven, 1995). However, it should be noted that the focus of this paper is on the fluid pressure regime during sedimentation, not on modeling the process of uranium mineralization. Nevertheless, the results of the present study have important implications for fluid flow models related to uranium mineralization, which are discussed in this paper.

2. Geological background

The Athabasca basin is composed of flat-lying Paleoproterozoic to Mesoproterozoic sedimentary rocks of the Athabasca Group, underlain by strongly deformed Archean to Paleoproterozoic metamorphic rocks in the basement (Jefferson et al., 2007). The unconformity between the basin and basement is marked by a paleo-weathering profile of variable thicknesses developed at the top of the basement (Jefferson et al., 2007). Typically, uranium mineralization occurs in basement rocks immediately below and in sandstones immediately above the unconformity, although mineralization 10s to 100 s of meters below the unconformity has been discovered.

2.1. Basement rocks

The basement rocks belong to, from west to east, the Taltson magmatic zone, the Rae Province, and the Hearne Province, the latter two forming the Churchill Province and being separated by the Snowbird tectonic zone (Fig. 1; Card et al., 2007). The Taltson magmatic zone, considered to be the southern extension of the Thelon tectonic zone, which separates the Rae Province from the Slave Province to the west (Hoffman, 1988), is composed of a variety of 1.99–1.92 Ga plutonic rocks intruding 3.2–2.14 Ga metamorphic complexes of amphibolite to granitic gneiss (Card et al., 2007). In Saskatchewan, the Rae Province is divided into several domains including Beaverlodge, Zemlak, Tantato, Lloyd, and Clearwater, whereas the Hearne Province comprises the Virgin River, Mudjatik, Wollaston and Peter Lake domains, which are bounded by the Trans-Hudson Orogen to the east (Fig. 1; Card et al., 2007). Both the Rae and Hearne provinces in Saskatchewan contain ca. 3.0 Ga granitoid gneiss and >2.6 Ga metasedimentary rocks (mainly in Rae) and metavolcanic rocks (mainly in Hearne), followed by Paleoproterozoic metasedimentary rocks, which are divided into the Murmac Bay, Thluicho Lake and Martin groups in Rae, and the Hurwitz Group and partly coeval Wollaston Supergroup in Hearne (Card et al., 2007). Paleoproterozoic metasedimentary rocks contain graphitic metapelitic units, mainly in the lower part of the Wollaston Supergroup in the Hearne Province, and in the Rae Province. Paleoproterozoic granitic intrusions with ages similar to those in the Taltson–Thelon and Trans-Hudson orogens are common in the Rae and Hearne provinces, respectively.

2.2. Sedimentary rocks in the Athabasca basin

The non-metamorphosed sedimentary rocks in the Athabasca basin belong to the Athabasca Group, which is divided into the following formations (from oldest to youngest): Fair Point, Read, Smart (may be a distal facies equivalent to Read), Manitou Falls, Lazenby Lake, Wolverine Point, Locker Lake, Otherside, Douglas, and Carswell (Fig. 1; Ramaekers et al., 2007). The Fair Point Formation is mainly composed of conglomerate and conglomeratic quartz arenite, with minor pebbly mudstone. The Read Formation consists of conglomerate and quartz arenite, with minor pebbly mudstone, and the Smart Formation of quartz arenite, with local pebbly mudstone. The Manitou Formation is composed of, from lower to upper, pebbly quartz arenite with >2% conglomerate in the Bird Member (MFb), pebbly and non-pebbly quartz arenite with >1% clay intraclasts in the Raibl Member (MFr), non-pebbly and pebbly quartz arenite with >1% clay intraclasts in the Warnes Member (MFw) (note: MFr and MFw are considered laterally equivalent to MFb), quartz arenite and pebbly quartz arenite in the Collins Member (MFc), and quartz arenite with >1% clay intraclasts in the Dunlop Member (MFd). The Lazenby Lake Formation consists mainly of quartz arenite, with siltstone and mudstone, and local conglomerate, and the Wolverine Point Formation comprises quartz arenite with abundant mudstone in the lower part. The Locker Lake Formation is composed of conglomeratic quartz arenite, and the Otherside Formation of quartz arenite and pebbly quartz arenite. The Douglas Formation consists of mudstone and fine to very fine quartz arenite, while the Carswell Formation comprises carbonates including stromatolitic to massive dolomite, stromatolite, and oolite with siliciclastic interbeds (Ramaekers et al., 2007). The Carswell Formation was formed in marginal marine environments, the Douglas Formation in playa lakes or lagoons, and the rest of the Athabasca Group were deposited in braided river systems (Ramaekers et al., 2007).

The lithostratigraphic units are grouped into 4 sequences separated by major unconformities: sequence 1 comprising the Fair Point Formation, sequence 2 of Read/Smart and Manitou Falls formations, sequence 3 of Lazenby Lake and Wolverine Point formations, and sequence 4 from Locker Lake to Carswell formations (Ramaekers et al., 2007). Based on the isopachs of the 4 sequences, the Athabasca basin is divided into 3 subbasins: the Jackfish subbasin in the west, where the Fair Point Formation (sequence 1) was deposited; the Cree subbasin in the east, where sequence 2 is thickest; and the Mirror subbasin in the mid-west, where sequences 2 and 3 are thickest (Figs. 1 and 2; Ramaekers et al., 2007). Sequence 1 is only exposed locally in the west margin of the basin, sequence 2 mainly in the east, and sequences 3 and 4 in the western part of the basin (Figs. 1 and 2; Ramaekers et al., 2007). The Douglas and Carswell formations only occur around the Carswell impact structure (Fig. 1; Ramaekers et al., 2007). Despite the overall west–east orientation of the Athabasca basin (Fig. 1), a number of "troughs" developed during the deposition history of the basin are oriented southwest–northeast, which is similar to the framework structures in the basement, suggesting multiple reactivations of the basement faults during the sedimentation in the basin (Jefferson et al., 2007). Provenance and sedimentary structure studies indicate that the sediments were derived from the east and south most of the time, except during the deposition of sequence 3, when the provenance was mainly from the south (Ramaekers et al., 2007).

The sedimentation in the Athabasca basin is inferred to have started after ca. 1750 Ma, based on a U–Pb titanite age of ca. 1752 Ma in the Wollaston domain (Annesley et al., 1997), $^{207}P/^{206}Pb$ and U–Pb rutile ages around 1750 Ma in the Mudjatik domain (Orrell et al., 1999), and the rapid erosion of the Trans-Hudson Orogen at ca. 1750 as indicated by Ar–Ar ages (Alexandre et al., 2009; Kyser et al., 2000). This age may represent the maximum age of the Fair Point Formation, while a younger age of 1740–1730 Ma has been suggested for the Manitou Falls Formation (Alexandre et al., 2009; Rainbird et al., 2006). An age of 1644 ± 13 Ma was reported for igneous zircon in tuffaceous units in the Wolverine Point Formation (Rainbird et al., 2007), and a Re–Os isochron age of 1541 ± 13 Ma was obtained for carbonaceous shales in the Douglas Formation (Creaser and Stasiuk, 2007). Microthermometric studies of fluid inclusions in authigenic quartz in sandstones from the Carswell structure and the Rumpel Lake drill core in the central part of the Cree subbasin suggest a paleogeothermal gradient of 35 °C/km and that more than 5 km of strata may have been eroded above the youngest preserved rocks in the basin (Pagel, 1975). The ages of these eroded strata are unknown, but they are likely older than the 1270 Ma mafic dikes (LeCheminant and Heaman, 1989) that cut the Athabasca Group and basement rocks. Also unknown are the ages and duration of the hiatuses between the different sequences.

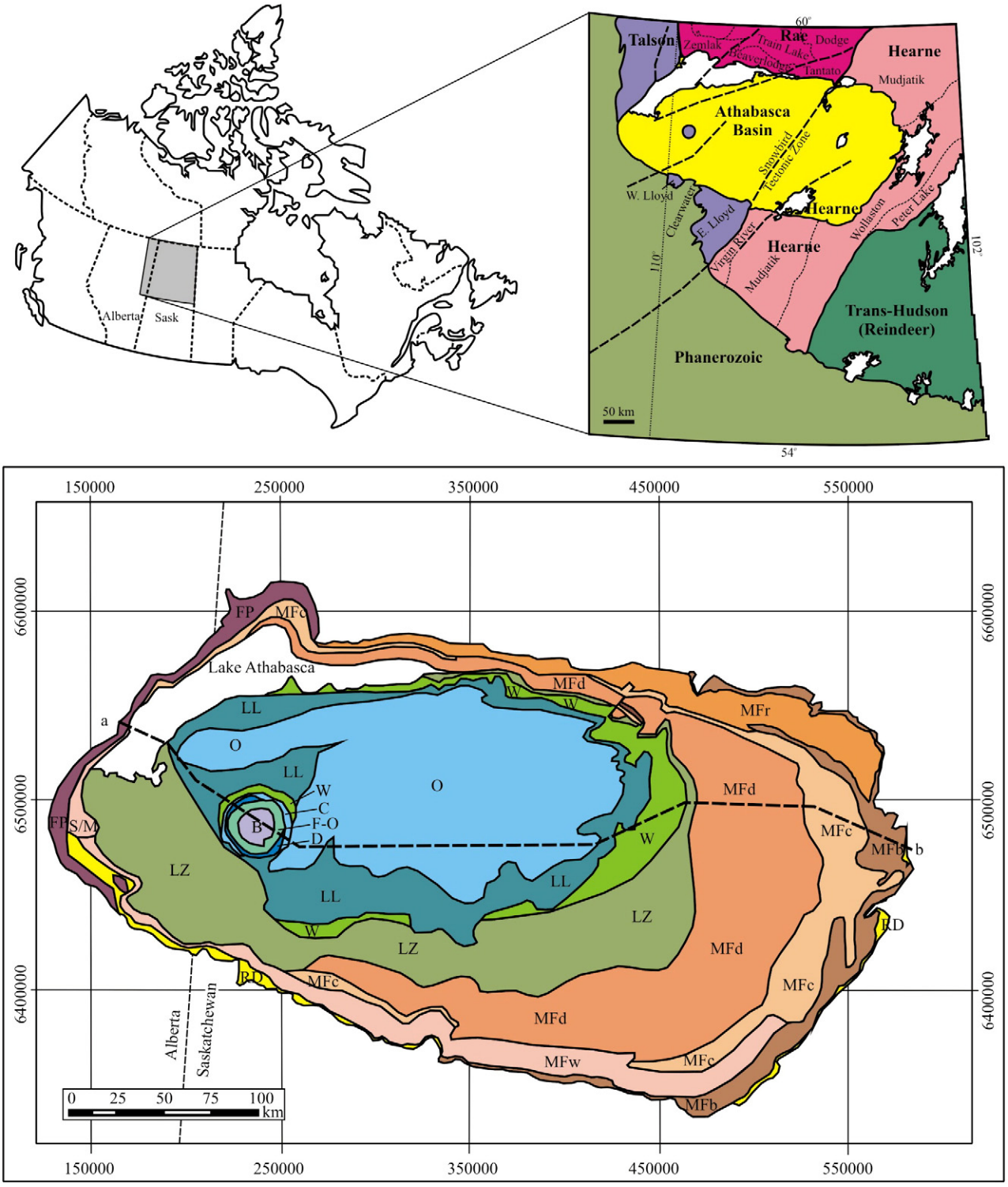

Fig. 1. B — basement; FP — Fair Point; S/M — undifferentiated Smart and/or Manitou Falls; RD — Read; MF — Manitou Falls (b — Bird; r — Raibl; w — Warnes; c — Collins; d — Dunlop); LZ — Lazenby Lake; W — Wolverine Point; LL — Locker Lake; O — Otherside; D — Douglas; C — Carswell; F–O — undivided Fair Point to Otherside formations. Dash line a–b indicates the location of the cross section shown in Fig. 2.
Upper: location and regional geologic framework of the Athabasca basin (modified from Card et al., 2007); lower: geological map of the Athabasca basin (modified from Ramaekers et al., 2007).

2.3. Uranium mineralization

Uranium deposits in the Athabasca basin occur near the unconformity with the basement and are associated with reactivated basement faults that cut and slightly displace the unconformity and are commonly but not exclusively graphite bearing (Jefferson et al., 2007; Kyser and Cuney, 2008). The mineralization is in massive and disseminated forms, and the average grade for all mined deposits is 2% U (with the highest grade of 22.28% U for the McArthur River deposit), which is five times the average grade of 0.4% of the Australian unconformity-related deposits (Jefferson et al., 2007; Kyser and Cuney, 2008). Some of the deposits are hosted in the sandstones of the Athabasca Group above the unconformity, named egress type, and some are in the basement below the unconformity, named ingress

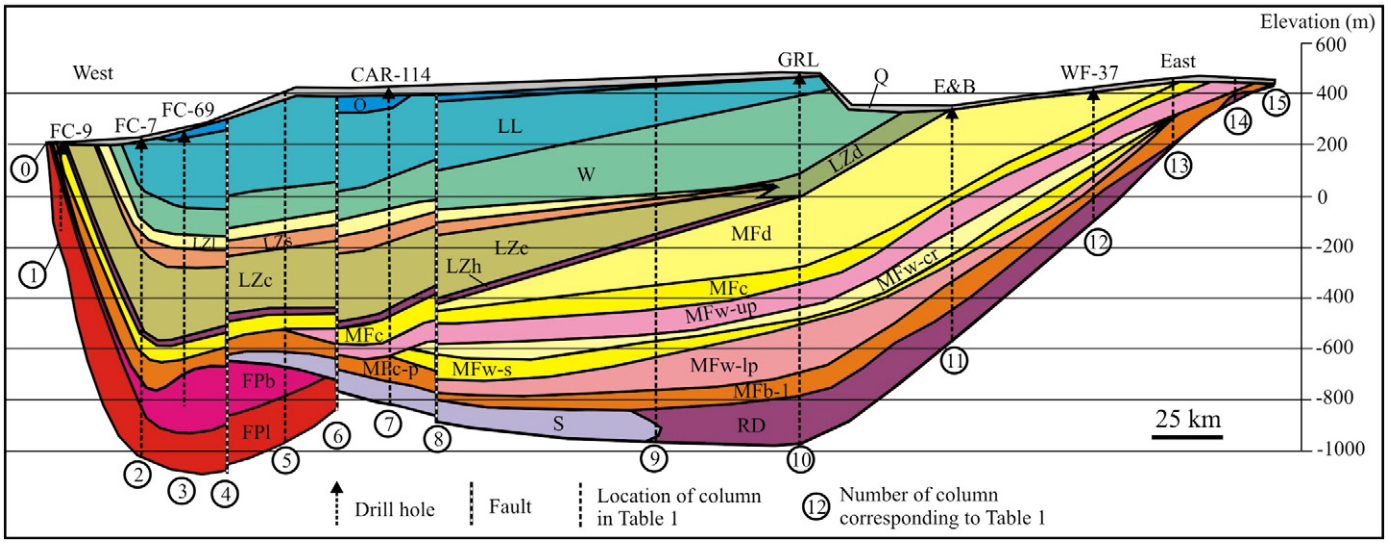

Fig. 2. The location of the cross section in the basin is shown in Fig. 1. FP — Fair Point; S — Smart; RD — Read; MF — Manitou Falls; LZ — Lazenby Lake; W — Wolverine Point; LL — Locker Lake; O — Otherside; D — Douglas; C — Carswell; Q — Quaternary.
A west–east cross section of the Athabasca basin (modified from Ramaekers et al., 2007).

type (Jefferson et al., 2007). The ingress-type deposits are controlled by steep to moderately-steep fractures and breccia zones, and characterized by relatively narrow alteration zones changing from illite-dominated outward to sudoite-dominated, and by relatively simple ore minerals (mainly uraninite), whereas the egress-type deposits have a flattened shape, bounded by extensive alteration zones changing from sudoite-dominated outward to illite-dominated, and characterized by polymetallic ores with significant concentrations of Ni, Co, Cu, Pb, Zn, and Mo in addition to U (Jefferson et al., 2007). The most important uranium deposits discovered so far are concentrated in the eastern margin of the basin, especially along the northeast-trending transition zone between the Mudjatik and Wollaston basement domains. The major uranium mineralization event is inferred to have occurred around 1590 Ma, based on LA-ICP-MS U–Pb dating of uraninite and Ar–Ar dating of syn-mineralization illite (Alexandre et al., 2009), although a spectrum of younger ages has been reported suggesting multiple uranium mineralization and/or uranium remobilization events (Jefferson et al., 2007; Kyser and Cuney, 2008).

3. The physical model and modeling methods

A two-dimensional (2D) model, based on the west–east cross section shown in Fig. 2, is constructed to represent the variation of sediment thickness across the basin, changes of lithologies between different strata, and the duration of sedimentation (Table 1). The strata are divided into the following hydro-stratigraphic units: 1) FPl (FP for Fair Point); 2) FPb; 3) Hiatus 1; 4) Smart-Read (S-R); 5) MFb-l (MF for Manitou Falls); 6) MFw-1p; 7) MFw-s; 8) MFw-cr; 9) MFw-up; 10) MFc; 11) MFd; 12) Hiatus 2; 13) LZh (LZ or Lazenby Lake); 14) LZc; 15) LZs; 16) LZl; 17) Wolverine Point (WP); 18) Hiatus 3; 19) Locker Lake (LL); 20) Otherside (O); 21) Douglas (D); 22) Carswell (C); and 23) Eroded strata (E). The thicknesses of the different units at different localities were measured from Fig. 2, and extrapolated where they are eroded, except for the Otherside, Douglas and Carswell formations, for which a maximum thickness of 183, 300 and 500 m (Ramaekers et al., 2007), respectively, was applied across the cross section. The hiatuses are represented by a thin layer of sediments of only one meter, and a thickness of 5000 m is assigned to the eroded strata above the Carswell Formation. The input thicknesses are expanded by the Basin2 program to account for the effect of compaction, with the factor of expansion being determined by iterative calculation. The start of sedimentation of the Fair Point Formation is set at 1750 Ma, as discussed above, and the end of sedimentation of the Carswell Formation at 1469 Ma as shown in Fig. 7 of Jefferson et al. (2007). A period of 50 Ma is arbitrarily assigned to the deposition of the assumed 5 km of eroded strata, so the ending time of sedimentation of the basin is 1419 Ma. The durations of individual hydrostratigraphic units are interpolated from these ages as well as the two ages obtained for the Wolverine Point Formation (1644 Ma) and the Douglas Formation (1541 Ma), as discussed above. Each of the hiatuses between the four sequences is assigned a duration of 2 million years. The lithologies of individual units are represented by different proportions of sandstone, shale and carbonate, mainly based on the data presented in Ramaekers et al. (2007). Rock porosity (φ) is related to effective depth (z_e) as described in Bethke (1985):

$$\varphi = \varphi_0 e^{-z_e b} + \varphi_1$$

where ϕ_0 is porosity at deposition, ϕ_1 is irreducible porosity, and b is an empirical parameter. Permeability (k) is related to porosity by

$$\log k_x = A\phi + B$$

where k_x is horizontal permeability, and A and B are lithology-dependent constants. Vertical permeability (k_z) is calculated from horizontal permeability with the ratio being a lithology-dependent constant. The porosity–depth and porosity–permeability relationship parameters are adopted from Harrison and Summa (1991) for sandstone and shale and from Kaufman (1994) for limestone (Table 2).

Variation studies were carried out to account for uncertainties of the lithologies, location and duration of the inferred eroded strata, as well as the influence of topographic relief. In the default model, the eroded 5 km strata, consisting of 50% sandstone and 50% shale, were deposited after the Carswell Formation over a period of 50 Ma. Different lithologic combinations (80% sandstone + 20% shale, and 20% sandstone + 80% shale) and sedimentation duration (30 Ma) were tested in the variation studies. Furthermore, a model with 5 km of strata (50% sandstone + 50% shale) being deposited between the Otherside and Douglas formations from 1636 to 1590 Ma and subsequently eroded from 1590 to 1570 Ma, followed by the deposition of the Douglas Formation, was examined to simulate the situation of uranium mineralization (1590 Ma) coinciding with maximum burial. A topographic relief of 500 m between the edges and the center of the basin, or between the two edges of the basin, was also tested to evaluate the influence of topography on fluid overpressure

Table 1
Lithology, time interval, and thickness of hydrostratigraphic units of the Athabasca basin as used in the numerical model.

Unit	Lithology	End time (Ma)	Thickness (m)[a]															
			0	1	2	3	4	5	6	7	8	9	10	11	12	13	14	15
Distance from the left boundary (km)			0	5.6	34.8	48.8	63.8	84.5	102.7	121.0	137.4	214.7	264.8	317.9	369.5	396.1	417.4	431.6
Eroded strata	50% ss + 50% sh	1419	5000	5000	5000	5000	5000	5000	5000	5000	5000	5000	5000	5000	5000	5000	5000	5000
Carswell	90% cn + 5% ss + 5% ah	1469	500	500	500	500	500	500	500	500	500	500	500	500	500	500	500	500
Douglas	30% ss + 70% sh	1541	300	300	300	300	300	300	300	300	300	300	300	300	300	300	300	300
Otherside	95% ss + 5% sh	1582	183	183	183	183	183	183	183	183	183	183	183	183	183	183	183	183
Locker Lake	95% ss + 5% sh	1602	100	150	203	267	293	329	307	259	260	153	93	90	85	80	75	70
Hiatus 3	100% ss	1642	1	1	1	1	1	1	1	1	1	1	1	1	1	1	1	1
Wolverine Point	40% ss + 60% sh	1644	35	35	89	106	115	121	111	123	155	268	296	250	230	210	190	170
Lazenby Lake																		
LZ l	98% ss + 2% sh	1652	30	30	34	59	63	65	63	54	45	15	12	10	10	10	10	10
LZs	98% ss + 2% sh	1654	10	15	40	77	59	56	57	58	48	24	20	15	15	15	15	15
LZc	98% ss + 2% sh	1656	100	112	150	261	234	232	269	240	233	112	44	45	50	45	40	40
LZh	98% ss + 2% sh	1666	15	15	20	22	25	25	26	28	28	20	20	10	10	10	10	10
Hiatus 2	100% ss	1667	1	1	1	1	1	1	1	1	1	1	1	1	1	1	1	1
Manitou Falls																		
MFd	97% ss + 3% sh	1669	0	0	0	0	0	0	0	0	32	180	268	282	260	240	220	200
MFc	99% ss + 1% sh	1689	40	43	50	58	60	60	61	89	72	95	63	37	42	44	50	50
MFw-up	97% ss + 3% sh	1694	0	0	0	0	0	0	54	54	71	92	92	84	59	68	66	60
MFw-cr	97% ss + 3% sh	1701	0	0	0	0	0	0	0	0	46	29	43	86	45	0	0	0
MFw-s	99% ss + 1% sh	1704	0	0	0	0	0	0	0	0	86	65	25	24	38	0	0	0
MFw-lp	99% ss + 1% sh	1706	0	0	0	0	0	0	0	0	46	126	184	66	40	0	0	0
MFb-l	99% ss + 1% sh	1720	10	15	78	59	49	79	51	69	44	71	87	93	32	72	21	20
Smart/ Read	95% ss + 5% sh	1727	0	0	0	0	0	22	58	77	91	126	179	96	71	0	15	0
Hiatus 1	100% ss	1740	1	1	1	1	1	1	1	1	1	1	1	1	1	1	1	1
Fair Point																		
FPb	97% ss + 3% sh	1742	8	8	66	228	190	118	0	0	0	0	0	0	0	0	0	0
FPl	97% ss + 3% sh	1746 1750	15	71	125	146	193	164	100		0	0	0	0	0	0	0	0

[a] Column number refers to those shown in Fig. 2; ss = sandstone, sh = shale, cn = carbonate.

and fluid flow. In order to evaluate the potential effect of early quartz cementation in the Manitou Falls Formation on fluid overpressure development, the unit of MFb-1 was assigned a lithology of 100% shale in a variation model to simulate an aquitard in the lower part of the Manitou Falls Formation, as proposed by Hiatt and Kyser (2007).

The left, right and upper boundaries are open to fluid flow, and the bottom boundary is impermeable. The surface temperature is fixed at 20 °C, and a heat flux of 71.8 mW/m^2 (or 1.715 HFU) is supplied from the bottom, which corresponds to a thermal gradient of 35 °C/km when an average thermal conductivity of 2.05 W/m °C (or 0.0049 cal/cm s °C) for a sedimentary rock of 10% porosity is used. Equations governing disequilibrium compaction, fluid flow and heat transfer were solved with the finite difference method, as described in Bethke (1985) and Bethke et al. (1993). Fluid salinity is assumed to be a constant equivalent to that of seawater. Although both continental and marine sediments were deposited in the Athabasca basin and basinal brines were involved in uranium mineralization, suggesting variable salinities, we are currently unable to characterize the distribution of salinities in space and time. Fluid density, viscosity, thermal expansion coefficient, compressibility coefficient, and heat capacity are related to temperature and pressure and calculated using data and equations compiled by Phillips et al. (1981), as elaborated by Bethke et al. (1993). The density and heat capacity of the rock are calculated as the weighted (based on porosity) average of the fluid and solid rock. The density of the solid is fixed at 2.65, 2.74, and 2.75 g/cm^3 for sandstone, shale, and carbonate, respectively, and the heat capacity of the solid is a function of temperature (Bethke et al., 1993). The thermal conductivity of the rock (K) is related to porosity (ϕ) by $K = 0.418\ (-4.4\ \phi + 5.35)$ W/m °C (or $(-4.4\ \phi + 5.35) \times 10^{-3}$ cal/cm s °C; Bethke et al., 1993).

Table 2
Constants related to porosity and permeability calculations.

Lithology	ϕ_0	ϕ_1	b[a]	A[a]	B[a]	k_x/k_z
Sandstone	0.40	0.05	0.50	15	−3	2.5
Shale	0.55	0.05	0.85	8	−8	10
Limestone	0.40	0.05	0.55	6	−4	2.5

[a] b is in km^{-1}, permeability calculated from A and B is in darcies.

4. Results of numerical modeling

The numerical modeling results for the base model (with the inputs outlined in Table 1) are shown as five snapshots (end of Fair Point, Manitou Falls, Wolverine Point, Carswell, and assumed eroded strata) in Fig. 3. From Fair Point to Carswell, fluid overpressures are close to zero (i.e., fluid pressures close to hydrostatic values), and fluid-flow vectors are upward and toward both margins of the basin. At the end of the assumed eroded strata, a maximum fluid overpressure of 32.5 bars was developed in the central part of the basin, causing downward fluid flow below the overpressured core, although fluid flow elsewhere is still upward and toward the margins of the basin (Fig. 3). However, the fluid pressures in the overpressured core are only slightly above hydrostatic values (Fig. 4). The maximum pore fluid factor (PFF = fluid pressure/lithostatic pressure) is 0.43, only slightly higher than the PFF of hydrostatic systems (0.4), and much lower than that of lithostatic systems (1.0). Maximum vertical fluid flow velocity was 0.0085 m/year, and maximum horizontal velocity was 0.075 m/year. Isotherms are flat

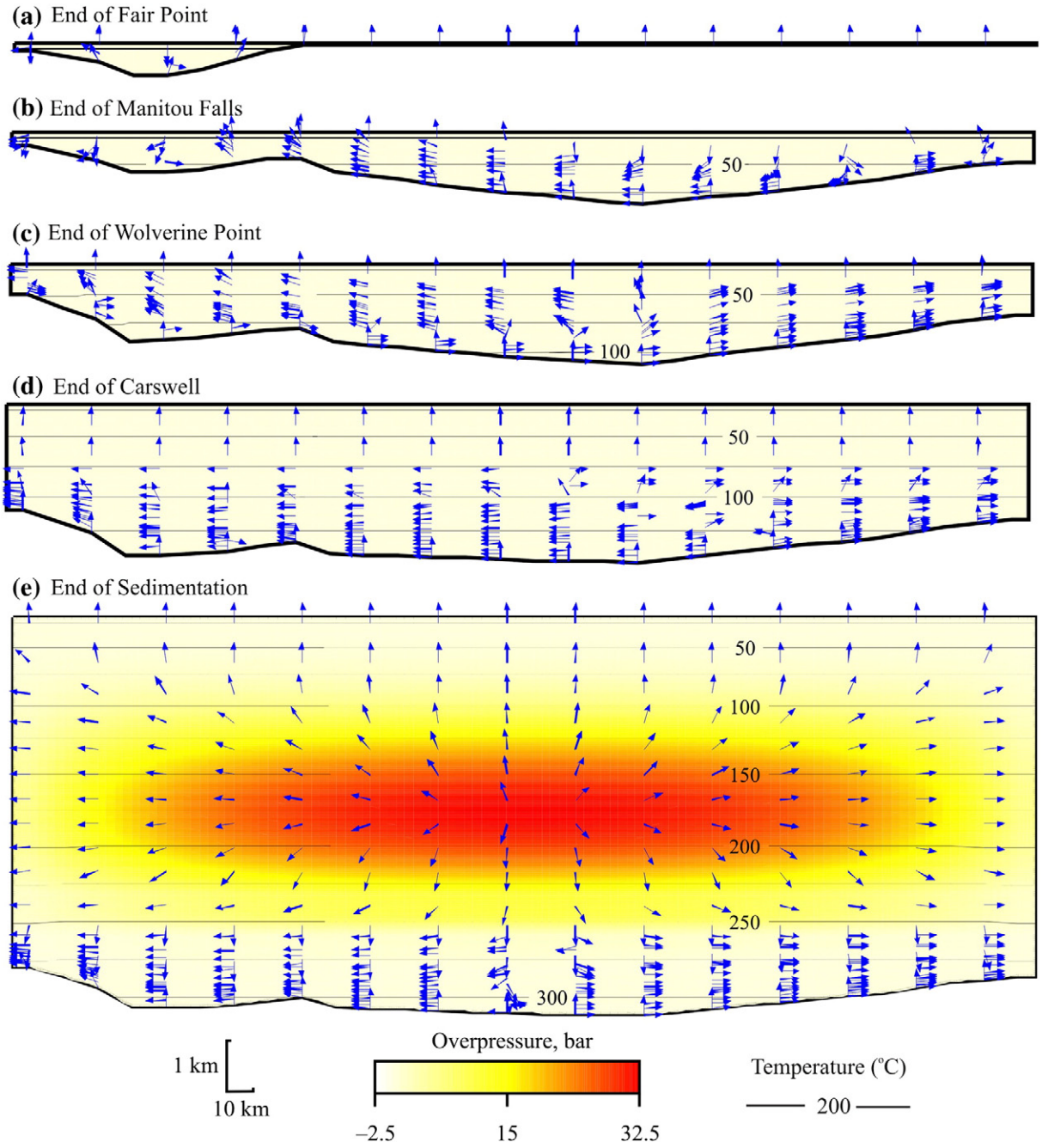

Fig. 3. Numerical modeling results of the base model (Table 1) showing fluid overpressure (bars, color scaled), fluid-flow direction (not to scale), and isotherms (°C) at the end of Fair Point (a), Manitou Falls (b), Wolverine Point (c), Carswell (d), and assumed eroded strata (e). No topographic relief is assigned on the surface.

throughout the sedimentation history (Fig. 3), suggesting that the upward and lateral fluid flow were not fast enough to disturb the thermal profile of the basin (Bethke, 1985).

The fluid overpressures in the assumed eroded strata decreased to a maximum of only 2.75 bars if the lithologies are approximated by 80% sand + 20% shale (as compared to the 50% sand + 50% shale in the base model) (Fig. 5a). On the other hand, the maximum fluid overpressure increased to 55 bars if the lithologies of the assumed eroded strata are represented by 20% sand and 80% shale (Fig. 5b). Reducing the duration of sedimentation of the assumed eroded strata from 50 Ma to 30 Ma also increased the fluid overpressures, to a maximum of 52.5 bars (Fig. 5c). However, none of these variation models have produced fluid pressures significantly above the hydrostatic values, with the maximum PFF being less than 0.49. Furthermore, the fluid-flow vectors and isotherm patterns (Fig. 5) are similar to those of the base model (Fig. 3).

Assuming 5 km of strata (50% sandstone + 50% shale) being deposited between the Otherside and Douglas formations, rather than after the Carswell Formation, produced similar fluid overpressure values and patterns (Fig. 6b) as the base model (Fig. 3e). The main difference is that in this modified model the maximum sediment thickness and fluid overpressure were achieved before the sedimentation of the

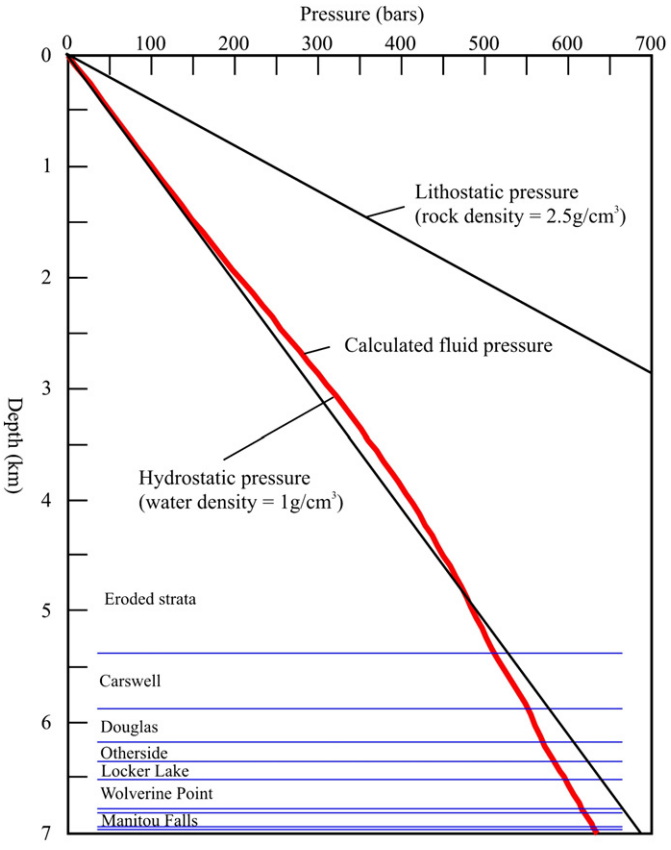

Fig. 4. Numerical modeling results showing the fluid pressure–depth profile in the central part of the basin at the end of sedimentation of the assumed eroded strata (same dataset as Fig. 3).

Douglas Formation, whereas in the base model these were achieved after the Carswell Formation. The fluid overpressure dramatically decreased after the erosion of the assumed 5 km strata, followed by sedimentation of the Douglas Formation (Fig. 6c).

Assuming a topographic relief of 500 m between the center and edge of the basin significantly changed the fluid-flow patterns and fluid overpressures, as shown by the snapshots for the end of the Carswell Formation (Fig. 7a) and the assumed eroded strata (Fig. 7b). Fluid flow is from basin margin toward basin center in the upper part of the basin, although it is still from basin center toward the margins in the lower part of the basin (Fig. 7). Fluid overpressures are significantly increased (relative to the base model) by this topographic effect, to a maximum of 65 bars at the end of the assumed eroded strata, and downward fluid flow is associated with this fluid overpressure core (Fig. 7b). Isotherms are not disturbed by the fluid flow, remaining parallel to the surface topography (Fig. 7).

If a topographic relief of 500 m is applied between the eastern (right) and western (left) margins, the fluid flow pattern becomes significantly different from all previous models; fluid flows from right to left at the end of the Carswell Formation (Fig. 8a), and mostly from right to left at the end of the assumed eroded strata (Fig. 8b). An overpressured core (maximum 32.5 bars) is also developed in the central part of the basin, with associated downward fluid flow (Fig. 8). Isotherms are parallel to the surface throughout the basin (Fig. 8).

In the variation model where MFb-1 was assigned a lithology of 100% shale to represent an aquitard, no perceivable effect on fluid overpressure development is observed. The maximum fluid overpressure was still 32.5 bars within the eroded strata, as in the base model (Fig. 3).

In all the variation studies, the maximum PFF value is less than 0.51, which is still close to the value of hydrostatic systems (0.4), and much lower than that of lithostatic systems (1.0). Therefore, the fluid pressure system in the Athabasca basin approximates a hydrostatic regime even if more impermeable lithologies than what are preserved in the basin are assumed or topographic relieves are included in the models.

5. Discussion

5.1. Fluid overpressure development and fluid pressure regime

The numerical modeling results indicate that only minor fluid overpressure was developed during the sedimentation history of the Athabasca basin. The validity of this evaluation is discussed in this section through examination of various mechanisms affecting fluid pressure regime and uncertainties related to the modeling.

Fluid overpressure in sedimentary basins can be caused by many mechanisms, including vertical deformation (compaction), horizontal deformation, aquathermal expansion, smectite dehydration, smectite to illite transformation, oil and gas generation, chemical compaction, hydraulic head from adjacent highland area, hydrocarbon buoyancy, and osmosis due to salinity variation (Swarbrick et al., 2002). Various studies have shown that among all these factors, disequilibrium compaction is by far the most important, and hydrocarbon generation may contribute to a lesser extent (e.g., Chi and Savard, 1998; Chi et al., 2010; Harrison and Summa, 1991; Osborne and Swarbrick, 1997; Swarbrick et al., 2002). The low fluid overpressure values in our numerical models are most likely attributed to two factors, the abundance of sandstones or scarcity of mudrocks and the low sedimentation rate, both facilitating fluid escape from pore space without being overpressured (Bethke, 1985; Swarbrick et al., 2002). The scarcity of mud in Proterozoic continental sediments may be partly related to the lack of plants (Kyser, 2007). The aquathermal expansion effect has already been considered in the Basin2 program, and its effect on fluid overpressure is known to be minor (Bethke, 1985). The content of organic matter in the Athabasca Group is generally low, with the highest TOC values being in the Douglas Formation, which are generally less than 1.5% (Wilson et al., 2007). This level of organic matter concentration, together with the maturation level being below gas generation conditions (Wilson et al., 2007), suggests that the contribution of hydrocarbon generation to fluid overpressure in the Athabasca basin is likely small. Topographic relief can increase fluid overpressure, as indicated by the model shown in Fig. 7, but the fluid overpressure (maximum 65 bars) is still sufficiently small so that the total fluid pressures are close to hydrostatic values. The effects of smectite dehydration, smectite to illite transformation, chemical compaction and osmosis on fluid overpressure have all been shown to be small compared to sediment compaction and hydrocarbon generation (Osborne and Swarbrick, 1997; Swarbrick et al., 2002).

Although we have carried out variation studies to address uncertainties on lithology and duration of the eroded strata, there are other uncertainties or factors that may affect the calculation results and that have not been considered in our numerical models, including the use of 2D rather than 3D models, ranges of porosity and permeability parameters, cementation and dissolution, lateral facies variation, and thermoelasticity of the framework grains. The potential effects of these factors on fluid overpressure development are further discussed here. In general the use of a 2D cross-sectional model to simulate a 3D basin is based on the assumption that the basin is symmetrical with respect to the location of the cross section such that there is no net fluid or heat flow across the cross section in the third dimension (i.e., in the direction perpendicular to the cross section). Previous studies suggest that a cross section running through the center of a basin, such as the one we used in this study (Fig. 1), may approximately satisfy the requirement of symmetry (e.g., Bethke, 1986; Harrison and Summa, 1991). The distribution of fluid overpressures predicted from this kind of 2D modeling in the Gulf of Mexico basin matches well present-day measurements (Harrison and Summa, 1991). Because parameters

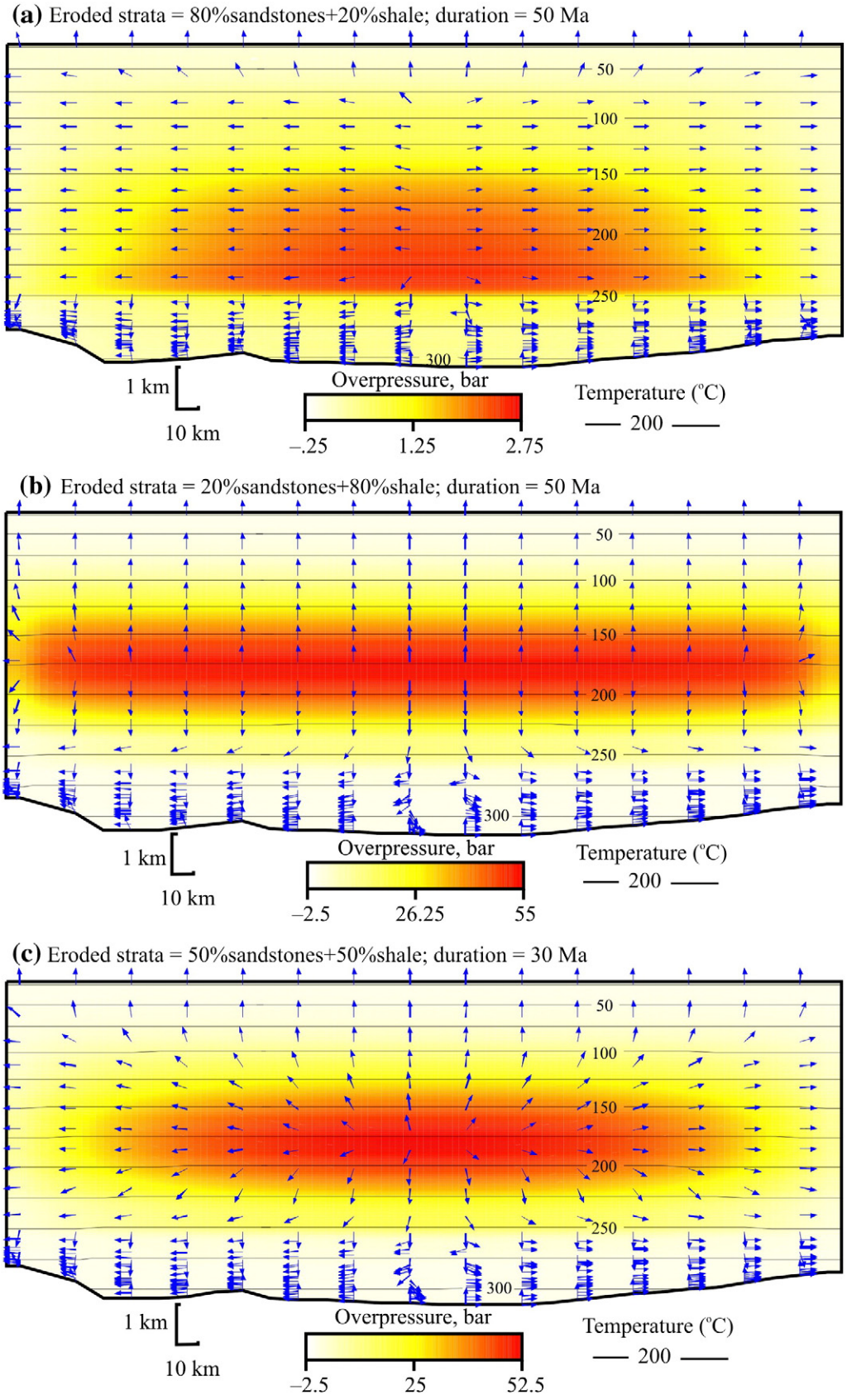

Fig. 5. Numerical modeling results showing fluid overpressure (bars, color scaled), fluid flow direction (not to scale), and isotherms (°C) at the end of sedimentation for different lithologies and duration for the assumed eroded strata: (a) eroded strata consist of 80% sandstone and 20% shale for a duration of 50 Ma; (b) eroded strata consist of 20% sandstone and 80% shale for a duration of 50 Ma; and (c) eroded strata consist of 50% sandstone and 50% shale for a duration of 30 Ma.

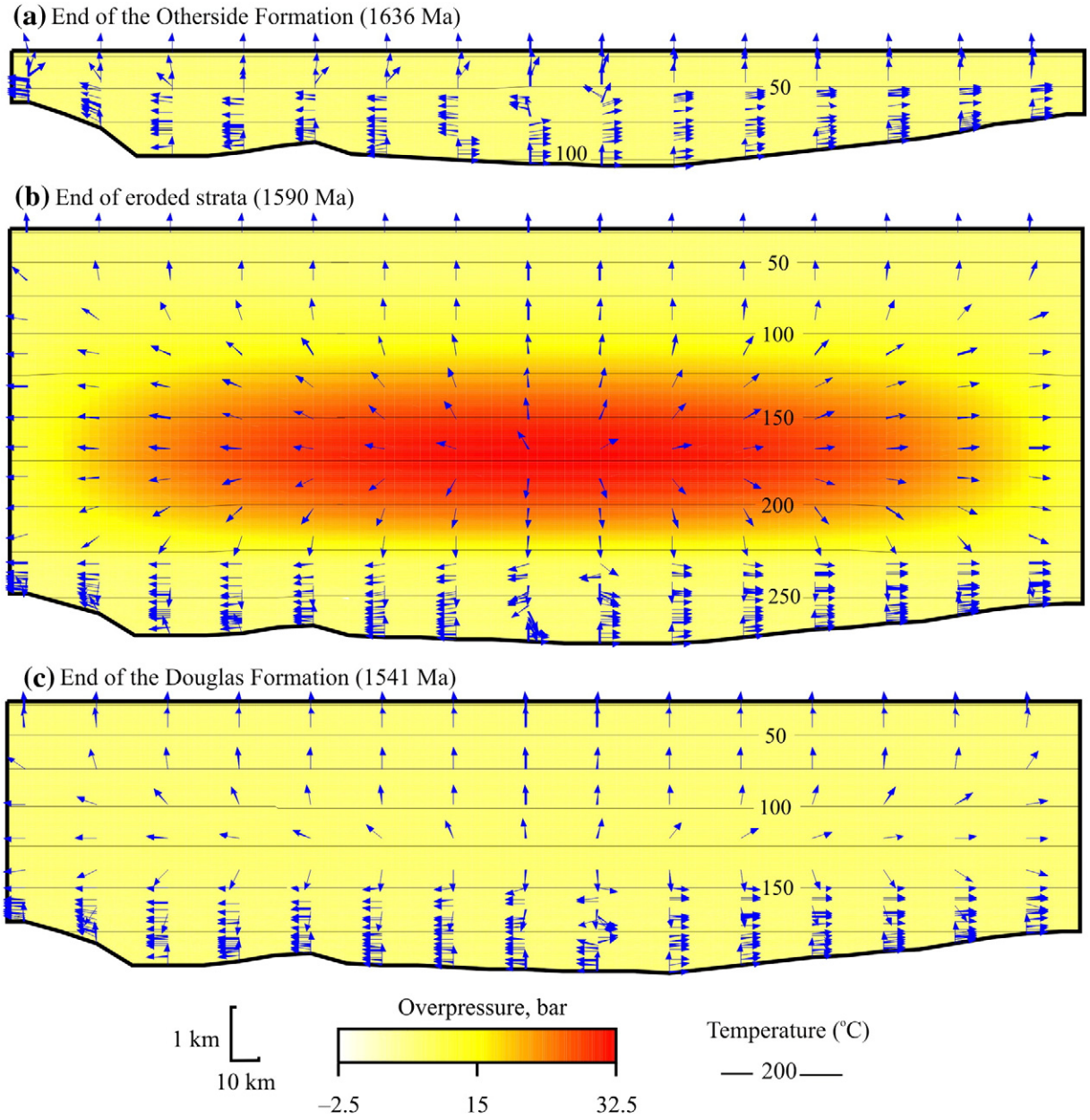

Fig. 6. Numerical modeling results showing fluid overpressure (bars, color scaled), fluid-flow direction (not to scale), and isotherms (°C) at the end of the Otherside Formation (a), the end of assumed 5 km strata that were deposited between Otherside and Douglas and subsequently eroded before deposition of Douglas (b), and at the end of Douglas (c).

related to porosity-permeability relationships specific to the Athabasca basin are not available, we have adopted parameters that are more conservative than those typical of sediments in intracraton basins (Bethke et al., 1993); specifically, we have used the same parameters as those of the Gulf of Mexico basin (Harrison and Summa, 1991) and the Maritimes basin (Chi and Savard, 1998), in which the permeability of shale is one order of magnitude lower than those of average shale (Bethke et al., 1993). Furthermore, the shale proportion (50%) assigned to the eroded strata is much higher than most of the preserved strata, meaning that we may have overestimated the fluid overpressure due to the low permeability of shales in our default model. Such overestimation is probably more than enough to counteract the effect of neglecting lateral facies variation (potentially higher proportions of shale toward basin center than the equivalent unit near the basin margin). Chemical processes can either generate porosity (dissolution) or reduce porosity (cementation), which has not been considered in our default model. Early quartz cementation has been recognized as an important diagenetic process that may have led to the formation of diagenetic aquitards (Hiatt and Kyser, 2007; Kyser, 2007). Our variation study using shale to simulate well-cemented sandstones in the Manitou Falls Formation suggests that the existence of such diagenetic aquitards has little effect on fluid pressure development. Furthermore, dissolution of framework grains may have counteracted the effect of cementation. Finally, our model has not considered the thermal expansion of the framework grains with increasing temperature, referred to as thermoelasticity (Zhao et al., 1999). Assuming a thermal expansion coefficient of 3×10^{-5}/°C for the framework grains (Zhao et al., 1999), the volume increase of framework grains by thermal expansion from the surface (20 °C) to the base of the Athabasca basin (315 °C) is 0.00885, which is two orders of magnitude smaller than the change of porosity due to compaction (about 0.5). Therefore, the effect of thermoelasticity on fluid overpressure development is negligible.

In summary, our estimation of the fluid pressure regime in the Athabasca basin being close to hydrostatic is possibly correct.

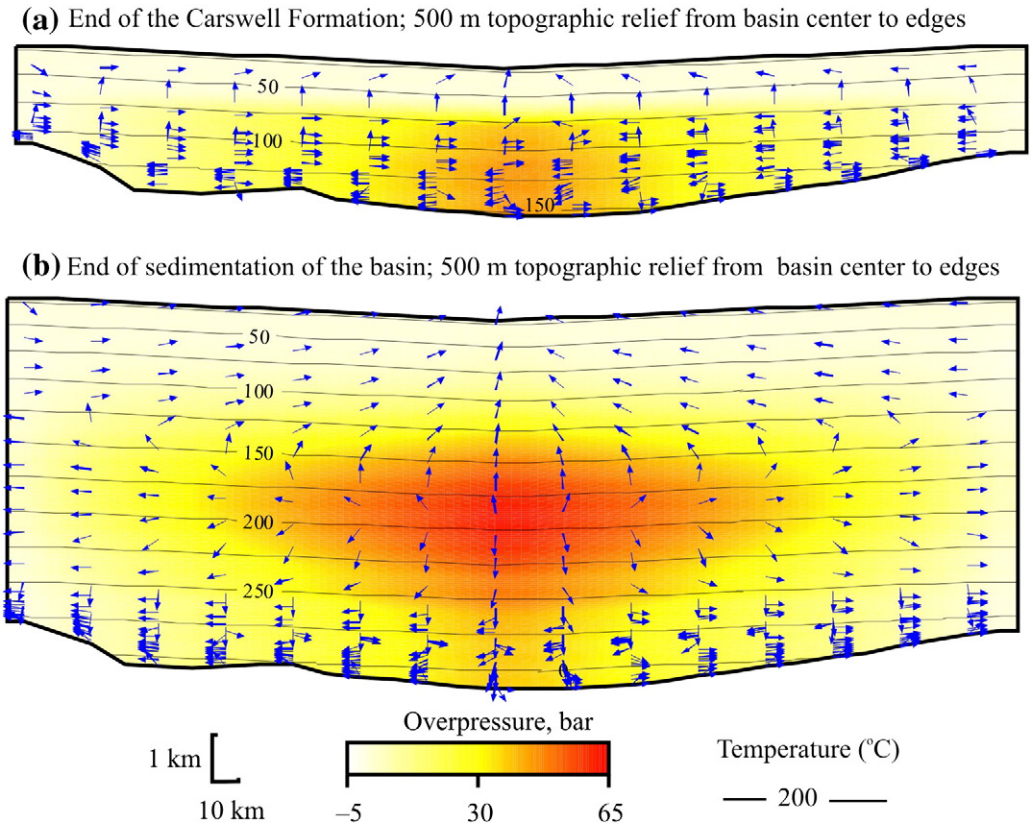

Fig. 7. Numerical modeling results showing fluid overpressure (bars, color scaled), fluid flow direction (not to scale), and isotherms (°C) at the end of sedimentation of the Carswell Formation (a) and the assumed eroded strata (b), assuming a topographic relief of 500 m between the edge and the center of the basin.

Mechanisms that would potentially produce higher fluid overpressure include hydrocarbon generation, cementation, clay mineral dehydration, lateral facies variation, and solid medium thermoelasticity, but the effect of these factors on overpressure development is likely to be small. On the other hand, the higher-than-normal proportion of shale and the lower-than-normal shale permeability in our models suggest that our models may have overestimated fluid overpressure. The overall low sedimentation rate and abundance of sandstones in the basin are the key factors leading to low fluid overpressure in the Athabasca basin, although local high fluid overpressure may have resulted from temporary and local high sedimentation rate and high shale proportion.

5.2. Implications for fluid flow models related to uranium mineralization

Although this study does not aim to directly model fluid-flow related to uranium mineralization in the Athabasca basin, the study results have important implications for such fluid-flow models. The formation of the high-grade uranium deposits near the unconformity requires large amounts of fluid flow through the sites of mineralization, which may be driven by fluid overpressure, topographic relief, density variation, and structural deformation (Chi and Xue, 2011). Fluid overpressure developed during sedimentation plays an important role in determining the overall fluid flow regime. Fluid flow driven by topographic relief and fluid convection driven by density variation are relatively easy to develop when the initial fluid-pressure system is near hydrostatic; strong fluid overpressure in the basin tends to suppress such fluid flow, although it has been shown that fluid convection is still possible in overpressured systems under certain conditions (Zhao et al., 2000). The mechanism of fluid flow related to structural deformation is also related to the fluid-pressure regime. In environments where the ambient fluid pressure is hydrostatic (such as in epithermal mineralization), fluid pressure may fluctuate between hydrostatic and hypo-hydrostatic values in response to fracturing, and fluid flow may be driven by the suction pump mechanism, whereas in environments in the hydrostatic–lithostatic transition zone (e.g., mesothermal mineralization), fluid pressure may fluctuate between hydrostatic and lithostatic values in response to episodic fracturing (earthquakes) and fluid pressure build up, as explained by the fault valve model (Sibson et al., 1988).

The numerical modeling results presented above indicate that fluid pressures in the Athabasca basin were close to hydrostatic values throughout the sedimentation history. This suggests that fluid flow driven by topographic relief (Alexandre and Kyser, 2012; Derome et al., 2005) or convection related to fluid density variation (Boiron et al., 2010; Hoeve and Sibbald, 1978; Raffensperger and Garven, 1995) are both theoretically plausible. However, our modeling results do not preclude other mechanisms including compaction-driven fluid flow (Hiatt and Kyser, 2007) and fluid flow related to structural deformation (Cui et al., 2012), because such fluid flow systems can also be developed in a near-hydrostatic background. Obviously, knowing that a fluid flow mechanism is possible in the Athabasca basin is insufficient to determine if this fluid flow mechanism was responsible for uranium mineralization. Other studies other than numerical modeling of fluid flow, such as measurement of basin-scale and deposit-scale thermal profiles using fluid inclusions and other thermal indicators (e.g., Chi et al., 1998; Leach and Rowan, 1986), and combined stress-fluid pressure studies using fluid inclusion planes (e.g., Liu et al., 2011), are required to discriminate these possible mechanisms.

Two other implications of the present study for uranium mineralization in the Athabasca basin are related to the localization of mineralization near the unconformity and the sources of the mineralizing fluids. The near-hydrostatic pressure regime in the basal part of the Athabasca basin is favorable for oxidizing fluids from the shallower part of the basin to flow downward to the unconformity

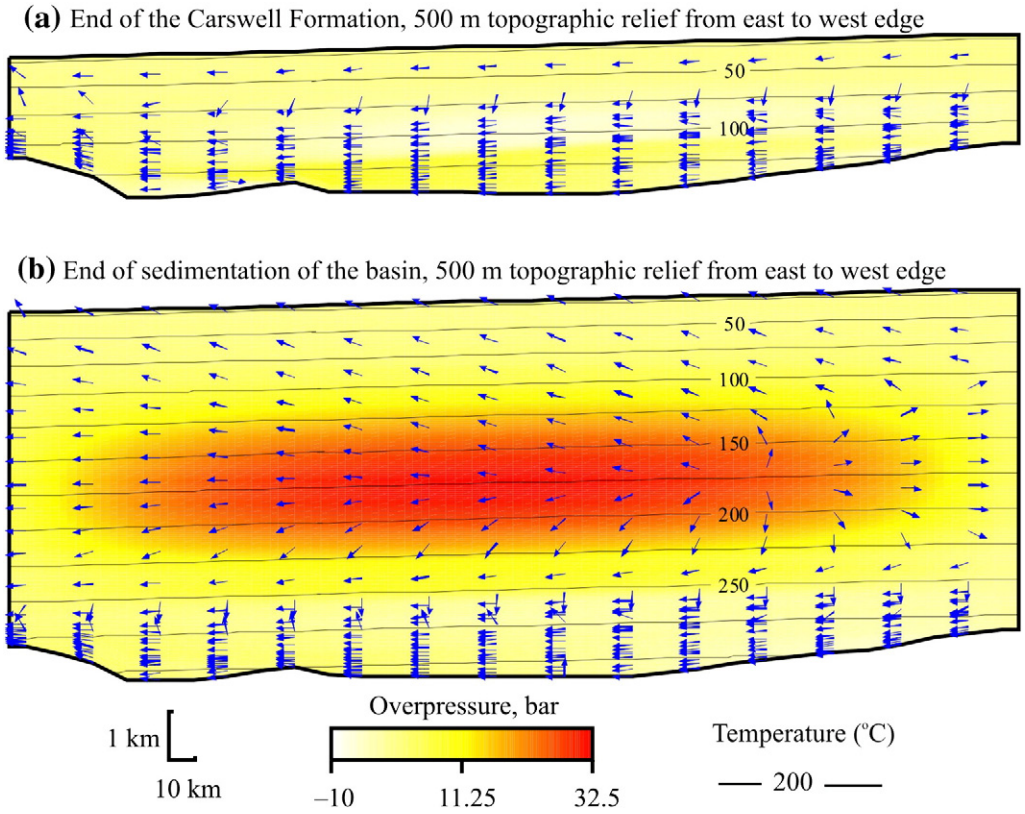

Fig. 8. Numerical modeling results showing fluid overpressure (bars, color scaled), fluid flow direction (not to scale), and isotherms (°C) at the end of sedimentation of the Carswell Formation (a) and the assumed eroded strata (b), assuming a topographic relief of 500 meters between the right and west edge of the basin.

through various mechanisms including compaction-driven flow, density-driven convection, and topography-driven flow. In contrast, strong fluid overpressure in the lower part of a basin, such as in the Gulf of Mexico basin (Harrison and Summa, 1991), would have prevented oxidizing fluids from penetrating deep into the base of the basin, thus limiting mineralization to the upper part of the basin (Chi, 2011). The downward fluid flow associated with the slightly elevated fluid overpressure in the assumed eroded strata (Figs. 3 and 5) is favorable for driving basinal brines derived from seawater evaporation in association with the Carswell Formation down to the basal part of the basin, and then laterally to the sites of mineralization toward basin margin, explaining the seawater evaporation origin of the mineralization fluids (Mercadier et al., 2012; Richard et al., 2011). The main difficulty of this model lies in the timing of the development of the assumed eroded strata and associated fluid overpressure (after the deposition of the Douglas Formation at about 1541 Ma; Creaser and Stasiuk, 2007) relative to the main phase of uranium mineralization (1590 Ma; Alexandre et al., 2009). However, it is not impossible that uranium mineralization started before maximum burial and then continued concurrently with more sedimentation, as reflected by the wide range of isotopic ages of uraninite (see Alexandre et al., 2009; Jefferson et al., 2007; Kyser and Cuney, 2008).

6. Conclusions

Numerical modeling of fluid pressure in the sedimentation history of the Athabasca basin indicates that the basin was near the hydrostatic regime or only very weakly overpressured. This is largely attributed to the sandstone-dominated lithologies of the basin and the prolonged sedimentation time. The results indicate that various fluid-flow models including compaction-driven flow, topographic relief-driven flow, convection due to density variation, and fluid flow related to faulting are all possible, a discrimination of which requires a better understanding of the geothermal profiles across the basin as well as around mineralization districts and individual deposits. It is suggested that the low fluid overpressure in the basal part of the basin may have been partly responsible for the development of unconformity-type uranium deposits, as higher fluid overpressures would have hindered the circulation of oxidizing fluids into the base of the basin and into the basement.

Acknowledgments

This study is supported by an NSERC-Discovery grant (to Chi) and by the Saskatchewan Ministry of Energy and Resources (to Bosman and Card). Constructive comments by three anonymous reviewers and associate editor Dr. David Huston have been helpful in improving the paper.

References

Alexandre, P., Kyser, T.K., 2012. Modeling of the fluid flow involved in the formation of Athabasca basin unconformity-type uranium deposits. Geological Association of Canada—Mineralogical Association of Canada Annual Conference Abstracts, vol. 35, p. 3.
Alexandre, P., Kyser, K., Polito, P., Thomas, D., 2005. Alteration mineralogy and stable isotope geochemistry of Paleoproterozoic basement-hosted unconformity-type uranium deposits in the Athabasca Basin, Canada. Economic Geology 100, 1547–1563.
Alexandre, P., Kyser, K., Thomas, D., Polito, P., Marlat, J., 2009. Geochronology of unconformity-related uranium deposits in the Athabasca Basin, Saskatchewan, Canada and their integration in the evolution of the basin. Mineralium Deposita 44, 41–59.
Annesley, I.R., Madore, C., Shi, R., Krogh, T.E., 1997. U–Pb geochronology of thermotectonic events in the Wollaston Lake area, Wollaston Domain: a summary of 1994–1996 results. Summary of Investigations 1997. Saskatchewan Geological Survey, Saskatchewan Energy and Mines, Miscellaneous Report 97-4, pp. 162–173.
Bethke, C.M., 1985. A numerical model of compaction-driven groundwater flow and heat transfer and its application to paleohydrology of intracratonic sedimentary basins. Journal of Geophysical Research 90, 6817–6828.
Bethke, C.M., 1986. Hydrologic constraints on the genesis of the Upper Mississippi Valley mineral district from Illinois basin brines. Economic Geology 81, 233–249.

Bethke, C.M., Lee, M.K., Quinodoz, H., Kreiling, W.N., 1993. Basin Modeling with Basin2, a Guide to Using Basin2, B2plot, B2video, and B2view. University of Illinois, Urbana . 225 pp.

Boiron, M.-C., Cathelineau, M., Richard, A., 2010. Fluid flows and metal deposition near basement/cover fluid flows and metal deposition near basement /cover unconformity: lessons and analogies from Pb–Zn–F–Ba systems for the understanding of Proterozoic U deposits. Geofluids 10, 270–292.

Card, C.D., Pana, D., Portella, P., Thomas, D.J., Annesley, I.R., 2007. Basement rocks of the Athabasca basin, Saskatchewan and Alberta. In: Jefferson, C.W., Delaney, G. (Eds.), EXTECH IV: geology and uranium exploration technology of the Proterozoic Athabasca Basin, Saskatchewan and Alberta: Geological Survey of Canada Bulletin, 588, pp. 69–87.

Chi, G., 2011. Hydrodynamic control on localization of uranium deposits in sedimentary basins. Geological Society of America Annual Conference (October 9–12, Minneapolis), Abstracts with Programs, vol. 43, p. 667.

Chi, G., Savard, M.M., 1998. Basinal fluid flow models related to Zn–Pb mineralization in the southern margin of the Maritimes Basin, eastern Canada. Economic Geology 93, 896–910.

Chi, G., Xue, C., 2011. An overview of hydrodynamic studies of mineralization. Geoscience Frontiers 2, 423–438.

Chi, G., Kontak, D.J., Williams-Jones, A.E., 1998. Fluid composition and thermal regime during base-metal mineralization in the lower Windsor Group, Nova Scotia. Economic Geology 93, 883–895.

Chi, G., Lavoie, D., Bertrand, R., Lee, M.K., 2010. Downward hydrocarbon migration predicted from numerical modeling of fluid overpressure in the Paleozoic Anticosti Basin, eastern Canada. Geofluids 10, 334–350.

Chi, G., Bosman, S., Card, C., 2011. Fluid flow models related to uranium mineralization in the Athabasca basin: a review and new insights. Saskatchewan Geological Survey Open House 2011, Saskatoon, Abstract Volume, p. 4.

Creaser, R.A., Stasiuk, L.D., 2007. Depositional age of the Douglas Formation, northern Saskatchewan, determined by Re–Os geochronology. In: Jefferson, C.W., Delaney, G. (Eds.), EXTECH IV: geology and uranium exploration technology of the Proterozoic Athabasca Basin, Saskatchewan and Alberta: Geological Survey of Canada Bulletin, 588, pp. 341–346.

Cui, T., Yang, J., Samson, I.M., 2012. Tectonic deformation and fluid flow: implications for the formation of unconformity-related uranium deposits. Economic Geology 107, 147–163.

Cuney, M., Brouand, M., Cathelineau, M., Derome, D., Freiberger, R., Hecht, L., Kister, P., Lobaev, V., Lorilleux, G., Peiffert, C., Bastoul, A.M., 2003. What parameters control the high-grade-large tonnage of Proterozoic unconformity related uranium deposits? Proceedings of International Conference on Uranium Geochemistry, Nancy, France, pp. 123–126.

Dahlkamp, F.J., 1978. Geological appraisal of the Key Lake U–Ni deposits, northern Saskatchewan. Economic Geology 73, 1430–1449.

Derome, D., Cathelineau, M., Cuney, M., Farbe, C., Lhomme, T., 2005. Mixing of sodic and calcic brines and uranium deposition at McArthur River, Saskatchewan, Canada: a Raman and laser-induced breakdown spectroscopic study of fluid inclusions. Economic Geology 100, 1529–1545.

Fayek, M., Kyser, T.K., 1997. Characterization of multiple fluid-flow events and rare-earth-element mobility associated with formations of unconformity-type uranium deposits in the Athabasca Basin, Saskatchewan. The Canadian Mineralogist 35, 627–658.

Harrison, W.J., Summa, L.L., 1991. Paleohydrogeology of the Gulf of Mexico basin. American Journal of Science 291, 109–176.

Hetch, L., Cuney, M., 2000. Hydrothermal alteration of monazite in the Precambrian basement of the Athabasca Basin: implications for the genesis of unconformity-related deposits. Mineralium Deposita 35, 791–795.

Hiatt, E., Kyser, K., 2007. Sequence stratigraphy, hydrostratigraphy, and mineralizing fluid flow in the Proterozoic Manitou Falls Formation, eastern Athabasca Basin, Saskatchewan. In: Jefferson, C.W., Delaney, G. (Eds.), EXTECH IV: geology and uranium exploration technology of the Proterozoic Athabasca Basin, Saskatchewan and Alberta: Geological Survey of Canada Bulletin, 588, pp. 489–506.

Hoeve, J., Quirt, D.H., 1984. Uranium Mineralization and Host–Rock Alteration in Relation to Clay Mineral Diagenesis and Evolution of the Middle Proterozoic Athabasca Basin, Northern Saskatchewan, Canada. Technical Report 187. Saskatchewan Research Council. 187 pp.

Hoeve, J., Sibbald, T., 1978. On the genesis of Rabbit Lake and other unconformity-type uranium deposits in northern Saskatchewan, Canada. Economic Geology 73, 1450–1473.

Hoeve, J., Sibbald, T., Ramaekers, P., Lewry, J., 1980. Athabasca unconformity-type uranium deposits: a special class of sandstone-type deposits? In: Ferguson, S., Goleby, A. (Eds.), Uranium in the Pine Creek Geosyncline. IAEA, Vienna, pp. 575–594.

Hoffman, P.F., 1988. United plates of America, the birth of a craton: Early Proterozoic assembly and growth of Laurentia. Annual Review of Earth and Planetary Sciences 16, 543–603.

Jefferson, C.W., Thomas, D.J., Gandhi, S.S., Ramaekers, P., Delaney, G., Brisban, D., Cutts, C., Portella, P., Olson, R.A., 2007. Unconformity-associated uranium deposits of the Athabasca Basin, Saskatchewan and Alberta. In: Jefferson, C.W., Delaney, G. (Eds.), EXTECH IV: geology and uranium exploration technology of the Proterozoic Athabasca Basin, Saskatchewan and Alberta: Geological Survey of Canada Bulletin, 588, pp. 23–67.

Kaufman, J., 1994. Numerical models of fluid flow in carbonate platforms: implications for dolomitization. Journal of Sedimentary Research 64, 128–139.

Kotzer, T., Kyser, T., 1995. Petrogenesis of the Proterozoic Athabasca Basin, northern Saskatchewan, Canada, and its relation to diagenesis, hydrothermal uranium mineralization and paleohydrogeology. Chemical Geology 120, 45–89.

Kyser, T.K., 2007. Fluids, basin analysis, and mineral deposits. Geofluids 7, 238–257.

Kyser, T.K., Cuney, M., 2008. Unconformity-related uranium deposits. In: Cuney, M., Kyser, M. (Eds.), Recent and not-so-recent developments in uranium deposits and implications for exploration: Mineralogical Association of Canada Short Course Series, 39, pp. 161–220.

Kyser, T.K., Hiatt, E., Renac, C., Durocher, K., Holk, G., Deckart, K., 2000. Diagenetic fluids in Paleo- and Meso-Proterozoic sedimentary basins and their implications for long protracted fluid histories. In: Kyser, T.K. (Ed.), Fluid and basin evolution: Mineralogical Association of Canada Short Course, 28, pp. 225–262.

Leach, D.L., Rowan, E.L., 1986. Genetic link between Ouachita foldbelt tectonism and the Mississippi Valley-type lead–zinc deposits of the Ozarks. Geology 14, 931–935.

LeCheminant, A.N., Heaman, L.M., 1989. Mackenzie igneous events, Canada: middle Proterozoic hotspot magmatism associated with ocean opening. Earth and Planetary Science Letters 96, 38–48.

Liu, Y., Chi, G., Bethune, K.M., Dube, B., 2011. Fluid dynamics and fluid–structural relationships in the Red Lake mine trend, Red Lake greenstone belt, Ontario, Canada. Geofluids 11, 260–279.

Mercadier, J., Richard, A., Cathelineau, M., 2012. Boron- and magnesium-rich marine brines at the origin of giant unconformity-related uranium deposits: $\delta^{11}B$ evidence from Mg-tourmalines. Geology 40, 231–234.

Oliver, N.H.S., McLellen, J.G., Hobbs, B.E., Cleverley, J.S., Ord, A., Feltrin, L., 2006. Numerical models of extensional deformation, heat transfer and fluid flow across basement–cover interfaces during basin-related mineralization. Economic Geology 101, 1–31.

Orrell, S.E., Bickford, M.E., Lewry, J.F., 1999. Crustal evolution and age of thermotectonic reworking in the western hinterland of Trans-Hudson Orogen, northern Saskatchewan. Precambrian Research 95, 187–223.

Osborne, M.J., Swarbrick, R.E., 1997. Mechanisms which generate overpressure in sedimentary basins: a reevaluation. AAPG Bulletin 81, 1023–1041.

Pagel, M., 1975. Détermination des conditions physico-chimiques de la silicification diagénétique des grès Athabasca (Canada) au moyen des inclusions fluids. Comptes Rendus de l'Académie des Sciences Paris 280, 2301–2304.

Phillips, S.L., Igbene, A., Fair, J.A., Ozbek, H., 1981. A technical databook for geothermal energy utilization. Lawrence Berkeley Laboratory Report LBL-12810. . 46 pp.

Raffensperger, J.P., Garven, G., 1995. The formation of unconformity type uranium ore deposits: 1. Coupled groundwater flow and heat transport modeling. American Journal of Science 295, 581–636.

Rainbird, R.H., Stern, R.A., Rayner, N., Jefferson, C.W., 2006. Ar–Ar and U–Pb geochronology of a Late Paleoproterozoic rift basin: support for a genetic link with Hudsonian orogenesis, western Churchill Province, Nunavut, Canada. Journal of Geology 114, 1–17.

Rainbird, R.H., Stern, R.A., Rayner, N., Jefferson, C.W., 2007. Age, provenance, and regional correlation of the Athabasca Group, Saskatchewan and Alberta, constrained by igneous and detrital zircon geochronology. In: Jefferson, C.W., Delaney, G. (Eds.), EXTECH IV: geology and uranium exploration technology of the Proterozoic Athabasca Basin, Saskatchewan and Alberta: Geological Survey of Canada Bulletin, 588, pp. 193–209.

Ramaekers, P., Jefferson, C.W., Yeo, G.M., Collier, B., Long, D.G.F., Drever, G., McHardy, S., Jiricka, D., Cutts, C., Wheatley, K., Catuneanu, O., Bernier, S., Kupsch, B., Post, R.T., 2007. Revised geological map and stratigraphy of the Athabasca Group, Saskatchewan and Alberta. In: Jefferson, C.W., Delaney, G. (Eds.), EXTECH IV: geology and uranium exploration technology of the Proterozoic Athabasca Basin, Saskatchewan and Alberta: Geological Survey of Canada Bulletin, 588, pp. 155–191.

Richard, A., Pettke, T., Cathelineau, M., Boiron, M.-C., Mercadier, M., Cuney, M., Derome, D., 2010. Brine–rock interaction in the Athabasca basement (McArthur River U deposit, Canada): consequences for fluid chemistry and uranium uptake. Terra Nova 22, 303–308.

Richard, A., Banks, D.A., Mercadier, J., Boiron, M.-C., Cuney, M., Cathelineau, M., 2011. An evaporated seawater origin for the ore-forming brines in unconformity-related uranium deposits (Athabasca Basin, Canada): Cl/Br and $\delta^{37}Cl$ analysis of fluid inclusions. Geochimica et Cosmochimica Acta 75, 2792–2810.

Sibson, R.H., Robert, F., Poulsen, K.H., 1988. High-angle reverse faults, fluid-pressure cycling, and mesothermal gold–quartz deposits. Geology 16, 551–555.

Swarbrick, R.E., Osborne, M.J., Yardley, G.S., 2002. Comparison of overpressure magnitude resulting from the main generating mechanisms. In: Huffman, A.R., Bowers, G.L. (Eds.), Pressure regimes in sedimentary basins and their prediction: AAPG Memoir, 76, pp. 1–12.

Tourigny, G., Quirt, D.H., Wilson, N.S.F., Wilson, S., Breton, G., Portella, P., 2007. Geological and structural features of the Sue C uranium deposit, McClean Lake area, Saskatchewan. In: Jefferson, C.W., Delaney, G. (Eds.), EXTECH IV: geology and uranium exploration technology of the Proterozoic Athabasca Basin, Saskatchewan and Alberta: Geological Survey of Canada Bulletin, 588, pp. 229–247.

Wilson, N.S.F., Stasiuk, S.L., Fowler, M.G., 2007. Origin of organic matter in the Proterozoic Athabasca basin of Saskatchewan and Alberta, and significance to unconformity uranium deposits. In: Jefferson, C.W., Delaney, G. (Eds.), EXTECH IV: geology and uranium exploration technology of the Proterozoic Athabasca Basin, Saskatchewan and Alberta: Geological Survey of Canada Bulletin, 588, pp. 325–339.

Zhao, C., Hobbs, B.E., Mühlhaus, H.B., 1999. Effects of medium thermoelasticity on high Rayleigh number steady-state heat transfer and mineralization in deformable fluid-saturated porous media heated from below. Computer Methods in Applied Mechanics and Engineering 173, 41–54.

Zhao, C., Hobbs, B.E., Mühlhaus, H.B., 2000. Finite element analysis of heat transfer and mineralization in layered hydrothermal systems with upward throughflow. Computer Methods in Applied Mechanics and Engineering 186, 49–64.

Zhao, C.B., Reid, L.B., Regenauer-Lieb, K., 2012. Some fundamental issues in computational hydrodynamics of mineralization: a review. Journal of Geochemical Exploration 112, 21–34.